

#Reviewer 3

We thank the reviewers for their valuable comments, which have been essential in improving our study. In response to feedback from several reviewers, we have optimized the parameterization of the advection-dispersion module, allowing us to use a more realistic dispersion coefficient. In the new version of the article, as detailed in the responses to the questions, we have provided a more precise explanation of the dispersion coefficient used. Additionally, a new section (Section 3.1) has been added, where we justify in detail the need to include sinks, as well as provide a thorough description of the sink parameter. All the results presented in the article have been updated to reflect the new simulations performed with the improved model version. Although these new simulations do not alter the results or discussion presented, they contribute to greater clarity and precision in the presentation of the findings.

Major comments:

- 1. The study is based on assumptions which need to be clearly stated in section 2. Please mention how processes such as vertical mixing at the edge of the salinity front, which can significantly influence salinity distribution across the estuary, are accounted for in the model. Include a discussion of the vertical structure of the salt wedge and related citations in the Introduction. The model is validated using salinity data collected at 2 m depth. Salt intrusions could be happening at deeper depths, which seem to be unaccounted for in this study. Please justify.**

Thank you for the comment.

We have added a paragraph in the Introduction that discusses the vertical salinity structure in the GRE. Lines 93-103 (revised manuscript version)

“The vertical salinity structure in the Guadalquivir estuary is characterized by intense mixing that prevents the formation of significant gradients in salinity and temperature, resulting in a homogeneous distribution of water properties (García-Luque et al., 2003; Díez-Minguito et al., 2012). The low average flow of the river, combined with the high tidal prism resulting from the wide tidal range and shallow channel depth, contributes to the Guadalquivir estuary being a well-mixed estuary with very low vertical gradients in salinity and temperature (García-Lafuente et al., 2012). This type of well-mixed estuary is characterized by a uniform distribution of salinity, facilitated by strong tidal currents that prevent stratification. Similarly, the vertical circulation shows a relatively uniform current pattern during low-flow periods, with no significant changes in velocity or flow direction at different depths (Losada et al., 2017). The hydrodynamic model presented by Sirviente et al. (2023), validated with different observations recorded both at the surface and at depth, shows that there are no significant variations in velocities at different depths; therefore, the presence of significant stratification is unlikely, which favors the homogeneous distribution of salinity in the water column.”

In well-mixed estuaries such as the Guadalquivir, during periods of low discharge (which occurs for most of the year and under which all the simulations in this study were performed), one can assume a homogeneity of salinity concentration in the water column; that is, the vertical salinity gradients will be very small. This allows us to use our 1D model and validate it with the observations obtained from the ship's thermosalinograph.

This can be demonstrated attending to the CTD profiles recorded in our campaigns.

The vertical mixing and the reduced salinity gradient are evidenced by the data recorded by the CTD during each campaign. CTD profiles were performed at the different sampling points shown in Figure 1 of the manuscript, allowing us to analyze the vertical behavior of the salinity. The figures below correspond to the vertical salinity profiles measured during the MG1, MG2 and MG3 campaigns.

For MG3, CTD profiles were taken at 1-hour intervals over two tidal cycles, for a total of 25 hours at each site. For the MG1 and MG2 campaigns, measurements were taken at 1-hour intervals for a maximum of 10 hours. The sampling points for MG3 are the same as those shown in Figure 1 of the manuscript, as is the case for MG2. However, for MG1 there are more CTD sampling points than shown in the figure. The points for MG1 shown in the CTD plots correspond exactly to the positions of MG2 (see Figure 1a of the manuscript). It should be noted that there are no vertical profiles available for MG1-1 and not all sampling stations have 10 profiles.

When analyzing the behavior of the vertical profiles, it can be observed that in MG3 the water column always remains mixed, showing only very slight vertical salinity gradients during certain hours. The MG3 figure shows that vertical mixing prevails during the tidal cycles. Similarly, during the MG2 and MG1 campaigns, a strong vertical mixing is observed throughout the water column at all CTD profiles in all points of the river.

This observation was essential in simplifying our approach, allowing us to adopt a one-dimensional (1D) model, assuming that the salt concentration is homogeneous throughout the water column. We would like to emphasize that this strong mixing behavior is not always characteristic of the estuary. This intense mixing occurs under low discharge regimes (> 70% of the year), where freshwater flow is minimal and tidal dominance is dominant (as in our study case). In scenarios with moderate or high discharge regimes, the vertical salinity gradient behaves differently, leading to stratification of the water column. Under such conditions, this model cannot be applied as it would underestimate the salinity levels.

The fact that the water column is so well mixed indicates that we can validate our simulations with data obtained at 2 m depth, since, as seen in the profiles, the variation throughout the water column is reduced, allowing us to state that there is vertical homogeneity.

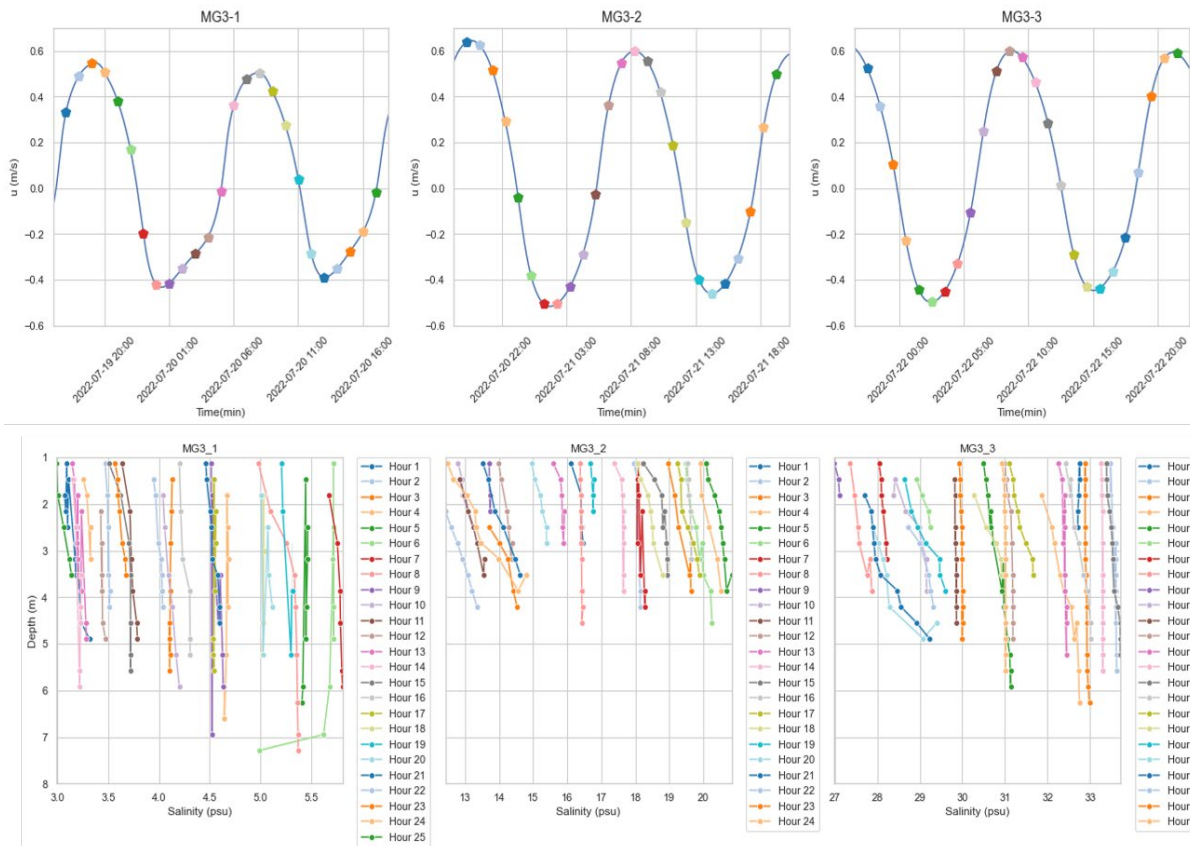


Fig. R1. The top panel corresponds to the tidal current velocity at each sampling station during the MG3 campaign (July 2022), with different colors indicating the tidal phases during which each CTD profile was taken. The bottom panel displays the CTD profiles at each sampling point along the Guadalquivir River during the MG3 campaign.

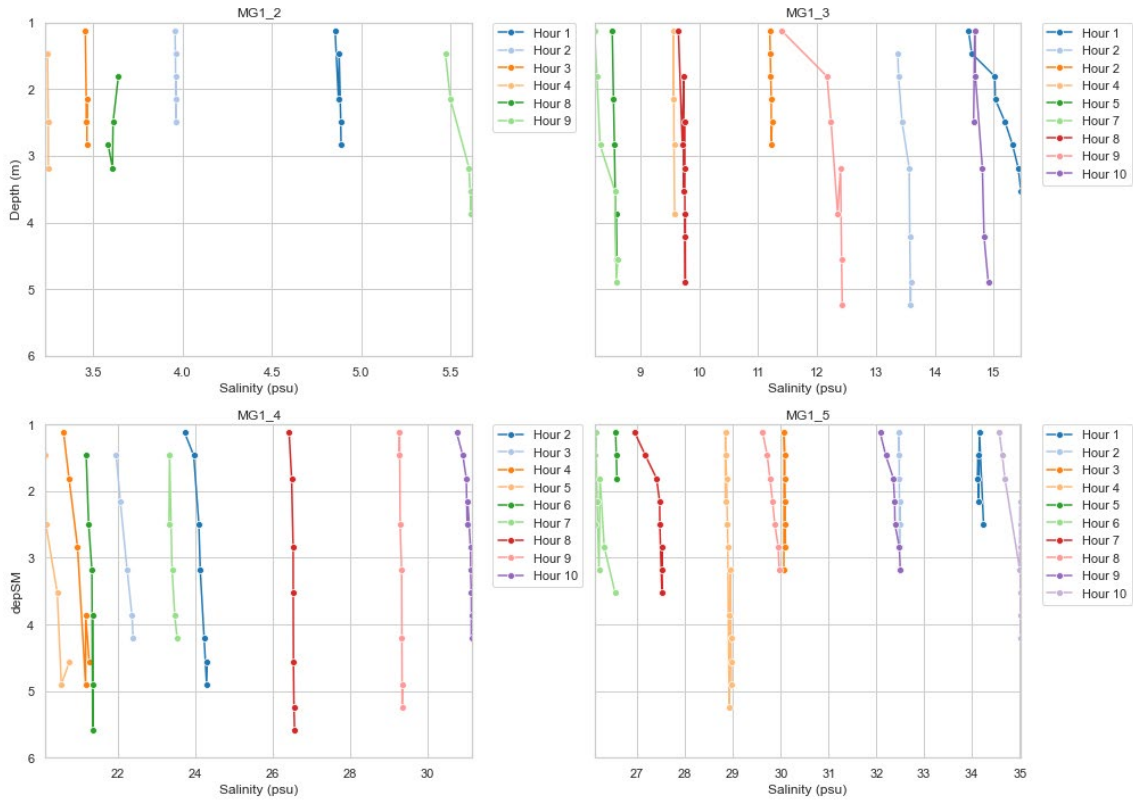


Fig. R2. CTD profiles at each sampling point along the Guadalquivir River during the MG2 campaign (January-February 2022).

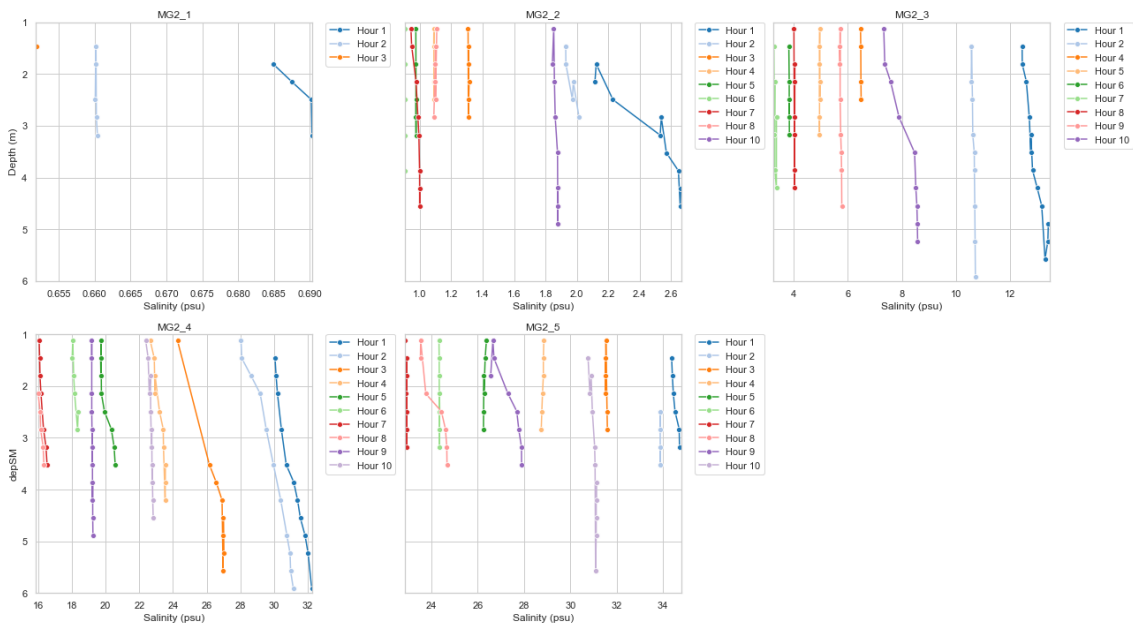


Fig. R3. CTD profiles at each sampling point along the Guadalquivir River during the MG1 campaign (September 2021).

2. Apart from the anthropogenic freshwater withdrawal, the sink term may also include uncertainties related to unaccounted processes such as drainage from marshes and crop lands, evaporation, vertical mixing etc. A strong justification on the attribution of sink term to anthropogenic effects has to be provided.

Thank you for your comment. We have included a new section (section 3.1) in order to provide a detailed explanation of why this sink parameter need to be included to simulate real behavior of salinity along the GRE and also a justification of what these parameter represent.

The GRE (Guadalquivir River Estuary) is under intense anthropogenic pressure, as evidenced by the reduction of marshland in recent decades, the expansion of agricultural fields - especially those dedicated to rice cultivation - and the development of urban areas adjacent to the river, among other factors. All these pressures are likely to affect the natural behavior of the GRE and may be one of the causes of the high salinity levels observed throughout the estuary.

One way of quantifying these impacts is in terms of water volume, as certain activities, such as agriculture or industry, withdraw water from the main channel and thereby affect it. In addition, it is important to consider contributions to the channel from smaller tributaries, agricultural fields and other sources.

In our study, the parameter δ plays a crucial role in quantifying the balance between water withdrawals and the smaller contributions that occur along the river. This allows us to attempt to quantify the impact of all potential activities in the GRE that can be assessed in terms of water volume.

The parameter δ is a key factor in quantifying the effect of extractions and minor contributions to water volume along the river. In other words, it represents all the natural and anthropogenic processes that can affect the volume of water, such as agricultural abstraction, industrial use, small side channels and evaporation. δ represents an average value between these two actions, and for our study it was positive, indicating that on average extractions exceed the contributions from smaller channels that drain into the main channel.

However, there is an inherent uncertainty in this parameter due to the complexity of accurately quantifying the amount of water extracted from the channel. The Guadalquivir system is heavily influenced by human activities (high levels of agriculture, industry, dense population in nearby areas, port activities, etc.), and it is also documented that numerous illegal extractions take place. This makes it difficult to obtain accurate data on abstraction within the estuary, as both the specific locations and volumes of water taken are unknown.

The main idea of this study is to show that these actions have a significant effect under low flow conditions, because without them the observed salinity levels would not be reached.

Thanks to the comments of the reviewers, we have reviewed the parameterizations and adapted the code to use higher dispersion values while maintaining the numerical stability of the model. This allowed us to perform a sensitivity analysis using a higher dispersion coefficient (150 m²/s) to evaluate whether the system could reproduce these observed salinity conditions with horizontal dispersion alone.

In this article, the horizontal dispersion coefficient was calculated using the equation proposed by Bowden (1983). This calculation was carried out for all the campaigns considered in the analysis to ensure the use of a constant dispersion appropriate to the system. The results indicate that the maximum constant dispersion, based on speed and depth, is 150 m²/s (this has also been added and explained in detail in the new version of the article). In addition, a sensitivity analysis was carried out with different dispersion coefficients to optimize this parameter as much as possible. In our 1D model, which simplifies the equations governing the balance forces, volume

conservation, and advection-dispersion processes, a dispersion coefficient exceeding 200 m²/s leads to numerical instabilities.

If we analyze the behavior of the horizontal salinity gradient along the estuary, taking into account only the horizontal dispersion, we can see that the system would never reproduce the observed salinity concentrations in the different campaigns. Even when the dispersion coefficient is increased to 190 m²/s, the behavior remains the same (Fig R4). It can be observed that, over time, the salinity concentration increases slightly from 10 km to 40 km. However, it is evident that the observed values are not fully reached. Therefore, it can be said that horizontal dispersion alone does not achieve the high salinity values observed along the channel, which opens the hypothesis that some additional effect is likely to cause a greater penetration of saline intrusion into the estuary.

If the same experiment is carried out but the parameter δ (representing all the processes that reduce the volume of water in the estuary) is included (Fig. R4), the results show that the system reaches the observed salinity values over time. This shows that this term must be included in order to reproduce the salinity concentrations observed in the different campaigns.

Figures 4c and 4d present the experiments that include water withdrawals as a constant value in time and space ($\delta = 0.005$ mm). As shown, as the simulation time progresses, the system achieves the salt concentrations range presented in the observations. This contrasts with the previous cases, where only the dispersion term was included in the experiments (Figures 4a and 4b), and the observed range could not be achieved.

On the other hand, Figures 4e and 4f show the experiments employing time-varying δ . In this simulation, a stronger sink is applied during the first three days ($\delta = 0.01$ mm), which is then reduced and held constant for the remainder of the simulation ($\delta = 0.001$ mm). In this case, the obtained values closely match those recorded in the observations.

These experiments highlight the necessity of including this term (δ) in the simulations, as otherwise, the horizontal salinity gradient would never reach the observed values. As illustrated in the figure, a certain duration of sink activity is required for the simulated salinity concentrations to approach the range observed. Therefore, it is essential to define an initial condition that considers this progression, allowing the simulation to adequately capture the evolution of the water withdrawals and their impact on salinity over time. This is particularly justified by Figures 4e and 4f, where using a stronger δ during the first three days followed by a weaker δ reproduces the observed behavior.

The δ value was determined empirically during the calibration process, through a sensitivity analysis in which different δ values were tested in simulations to identify the one that produced concentrations within the observed range while maintaining the temporal and spatial stability of the model.

Once the δ value was identified, experiments were carried out to analyze its behavior. These included constant use of the parameter over time, and experiments including them at specific time intervals, as well as spatial distribution experiments where δ was applied to specific points (e.g. high areas of the river) and regions. However, due to the limited understanding of the true behavior of these processes, and to avoid introducing assumptions or speculation that could affect the validity of the results, it was considered more appropriate to use a constant value rather than additional assumptions.

As observed, when sinks are included in the model, a certain amount of time is required for the system to reach the salinity concentrations observed. This behavior is represented in the model by an initial condition, designed as a logistic curve, which describes how the effect of the sinks manifests and evolves over a given period of time. This curve makes it possible to simulate the gradual adaptation of the system until it reaches the observed concentrations, providing a useful tool for evaluating and validating the model.

The choice of a logistic curve is justified by its ability to model gradual processes, which makes it suitable to reflect the temporal behavior of the sinks and their impact on the estuarine system. Therefore, the use of this parameter (δ) is an efficient way to quantify the inflows and outflows of water from the main channel, largely due to anthropogenic activities. This approach can be extrapolated to other estuaries with excessively high salinity concentrations in the estuary interior that cannot be explained by dispersion alone. Similarly, this method can be applied to systems under high anthropogenic pressure and similar environmental conditions.

In estuaries with behavior similar to that of the Guadalquivir River, especially in low flow conditions where the tidal action dominates the hydrodynamic behavior, the omission of the anthropogenic effect may lead to an underestimation of salinity concentrations. Therefore, including these effects through the δ parameter allows for more realistic simulations and helps to understand the impact of these activities. This understanding is essential for effective estuary management, both from a socio-economic and environmental perspective.

The results showed that δ is positive, indicating that, on average, water withdrawals exceed contributions to the main channel. This finding is consistent with documented evidence of significant anthropogenic impacts on the Guadalquivir system, including numerous illegal withdrawals that hinder the collection of accurate data (e.g. https://www.diariodesevilla.es/andalucia/Confederacion-Guadalquivir-ilegales-abastecian-hectareas_0_1844517515.html).

Our results provide an estimate of how these water withdrawals are occurring, but it is not possible to accurately quantify the exact behavior of water withdrawals due to anthropogenic activities or the exact volume diverted through secondary channels. What it does provide is a general view of the volume of water that needs to be abstracted during these campaigns, including all processes as a whole (including natural processes such as evaporation).

We believe that the use of the parameter δ is an efficient approach to quantifying the human impact on the system, particularly where there is a high degree of uncertainty in the actual abstraction activities. Furthermore, this methodology can be applied to other estuaries with significant anthropogenic pressures, providing a useful tool for dealing with similar situations of uncertainty.

The hydrodynamic model implemented, with its validation and detailed description available in Sirviente et al., 2023, inherently accounts for other anthropogenic effects, such as tidal amplification at the head of the estuary. Similarly, activities such as dredging and geometric modifications of the channel are considered by incorporating the actual bathymetry of the system

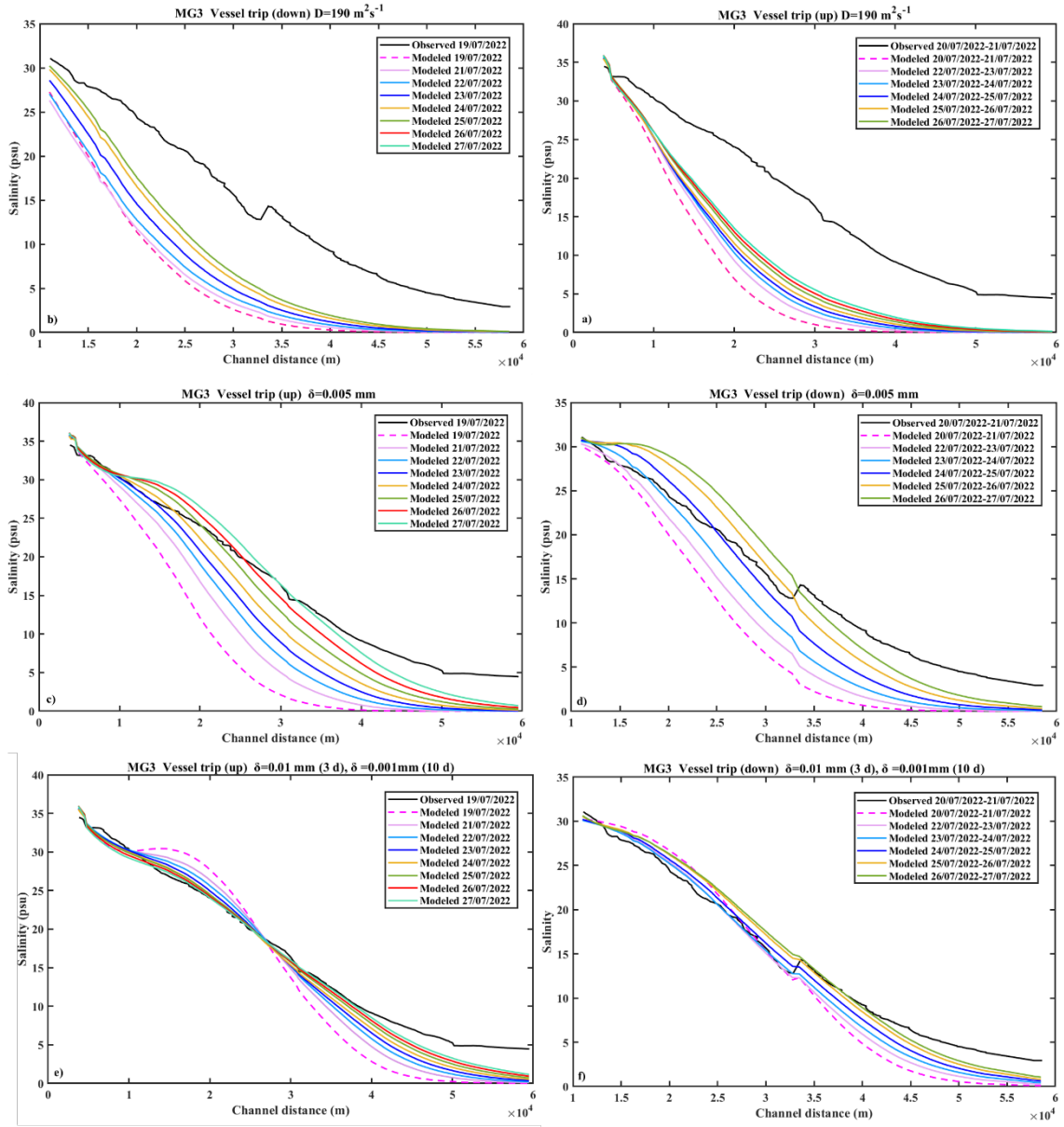


Fig. R4. Comparison of simulated (temporal behavior of the simulation at the corresponding observation points) and observed salinity over the MG3 vessel trips: (a) and (b) show simulations including only the horizontal dispersion for the MG3 vessel trip upstream (a) and downstream (b), with the observations in black. (c) and (d) show simulations incorporating δ term (δ) for the entire simulation period as constant value, and (e) and (f) are the simulation including a time-varying δ , compared to the observations (in black) for the MG3 vessel trip upstream (c and e) and downstream (d and f).

3. **Fig. 1b** shows that the channel is deep in the 15-25 km distance range, where the salt intrusions appear to be more pronounced (Figs. 5,6). It could be that the mixing induced by strong tidal currents at these depths result in increase in salinity, which is not related to freshwater withdrawal.

Indeed, in Figure 1b, between kilometers 15 and 25, some sections show greater depths. This graph reflects the actual bathymetry obtained from the nautical chart. Smoothing has been applied in the model to avoid discontinuities and to maintain homogeneity of the data.

In terms of vertical mixing induced by strong tidal currents, there is no significant difference between surface and bottom salinity. As mentioned in the answer to question 1, CTD profiles obtained during different campaigns show homogeneous vertical behavior, indicating that the vertical salinity gradient is practically constant, which implies that discrepancies between surface and bottom salinity are minimal.

In the revised version of the article, in which the model has been adapted as mentioned above, Figures 5 and 6 have been updated. This version presents a more realistic behavior and, by using a more accurate dispersion coefficient, the δ values are lower. Consequently, the increase observed in Figures 6b and 6d is smaller because the increase and decrease of the δ values used in the different experiments are smaller. However, the underlying concept and reasoning presented in the manuscript remain unchanged, although they have been adjusted to reflect these new results. In both figures, the time series of velocity and salinity are also included, overlaid for the Bonanza section (km 4), allowing the moments of maximum and minimum salinity concentration to be shown, as represented in Figures 5c-f and 6c-f.

New Figure 6 (Fig 5 in last manuscript version) and Figure 7 (Fig 6 in last manuscript version) of the manuscript are presented below:

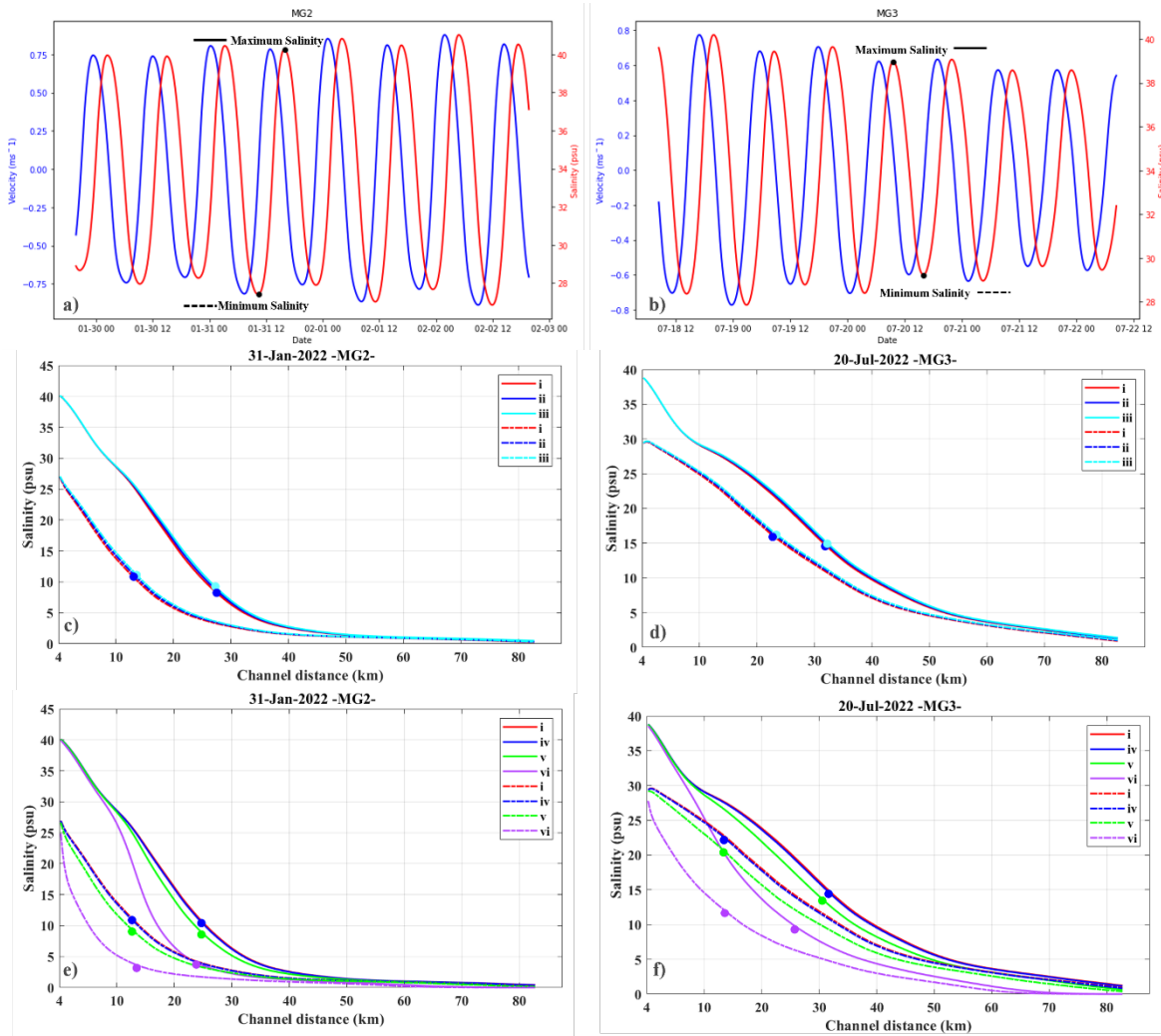


Figure 6. Superposition of current velocity (ms^{-1}) time series and Salinity (psu) time serie at Bonanza station (4 km). black dots mean maximum and minimum salinity moments selected for MG2 (a) and MG3 (b) oceanographic campaigns. Series of salinity (psu) along the Guadalquivir estuary (km) between real

flow and various reductions in freshwater flow for MG2 (c) and MG3 (d). In c and d, the red lines represent experiment (i), the blue lines correspond to experiment (ii) and the cyan lines are experiment (iii). (b) and (d) are the series of salinities using the real freshwater flow and greater freshwater flows for MG2 and MG3, respectively (Experiment (iv) is represented by the blue line, experiment (v) is green line and experiment vi is presented by pink lines). The solid lines represent the time of maximum salinity at Bonanza, and the dashed lines represent the time of minimum salinity at Bonanza. Color dots represent the km of maximum differences between each experiment with experiment (i).

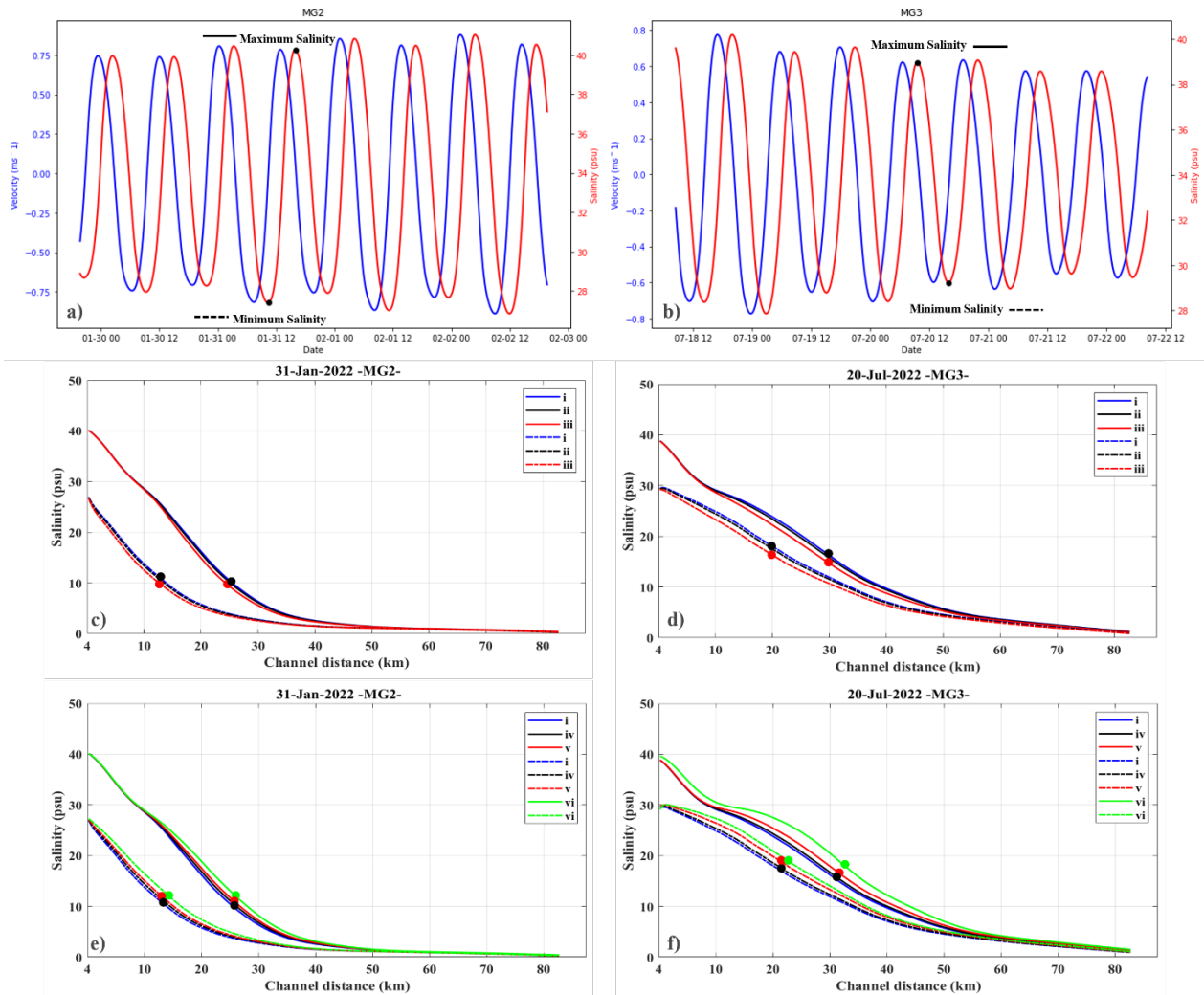


Figure 7: Superposition of current velocity (ms^{-1}) time series and Salinity (psu) time serie at Bonanza station (4 km). black dots mean maximum and minimum salinity moments selected for MG2 (a) and MG3 (b) oceanographic campaigns. Series of salinity (psu) along the Guadalquivir estuary (km) under a reduction of water withdrawals values are presented in (c) and (d) where original value are represented by blue lines (Experiment i), experiment (ii) corresponding to a smaller reduction is presented in black and a higher reduction of water withdrawal value is presented in red (Experiment (iii)). (e) and (f) correspond to experiments increasing water withdrawal values. Original value is presented in blue (Experiment i), and different progressive increases are presented by black lines (Experiment iv), red lines (Experiment v) and green lines (experiment vi). The solid lines represent the time of maximum salinity at Bonanza, and the dashed lines represent the time of minimum salinity at Bonanza. Color dots represent the km of maximum differences between each experiment with experiment (i).

In Figures 5 and 6, we consider that the areas where the changes are most significant are from km 10 to km 30, which could be due to several reasons. First, changes in width are likely to be more important than changes in depth. As shown in Figure 1c, there is a slight narrowing of the system from km 10 to about km 30, where the system widens slightly again. This narrowing could lead to an increase in current velocity, resulting in faster salt transport. However, these effects are not

the primary cause of the observed increase in saltwater intrusion. All simulations use the same bathymetry. One of the advantages of our model over previous models in the literature is that we do not use a channel with constant geometry. Instead, we use real bathymetry that includes changes in both depth and width. This means that our simulations inherently account for all physical processes, such as the Venturi effect due to the narrowing of the channel in certain areas.

As shown in the results presented in the article and in our response to comment 2, it is necessary to account for processes that lead to water volume reduction along the channel.

- 4. As noted by the other reviewers, there is confusion regarding the different terminology used for terms such as 'salt wedge' and 'salinity front'. Be consistent with the terminology and define a salt front/wedge. I guess it indicates the region where the lateral gradient in salinity is maximum. In Figs. 5,6 – Mark the location of maximum lateral change in salinity on each curve with a dot in respective color. It will be helpful for the readers to see the spatial variation in the salinity front in each model run.**

Thank you for the suggestion. We have added the corresponding dot to each line. This dot represents the kilometer where the discrepancy between the different experiments and the reference experiment (i) is at its maximum.

We have also corrected the terminology to be consistent through the text.

- 5. Observation data from the cruises are gathered in different months, ranging between July-February each year. I'm assuming the anthropogenic water withdrawals do not vary much across these months. Please mention that in the data section.**

In fact, the observations belong to different oceanographic campaigns carried out in different months and years. Specifically, we have observations from September 2021, January-February 2022, July 2022, and October 2023. Table 1 provides a summary of all observations, including their corresponding dates.

Regarding the sinks, as noted in response to comment 2, the parameter δ has very similar values across all simulations. For MG1, δ is set to 0.0015 mm. For MG2, the sink increases at certain distances: from 0 km to 22 km, $\delta = 0.0005$ mm; from 22 km to 42.250 km, $\delta = 0.0045$ mm; and from 42.250 km to 85 km, $\delta = 0.0005$ mm. For MG3, δ is 0.00225 mm, and for MG4, δ is 0.0012 mm.

This information is included in Section 3.3 because it was obtained experimentally through a sensitivity analysis, as mentioned in response to comment 2. We believe that including it in the data section could cause confusion among readers and lead them to interpret these values as direct observations.

Lines 206 (revised manuscript version):

“To account for water volume withdrawals from the estuary, a parameter called “sink” (denoted by δ) was introduced. It represents the thickness (m) of a water slide of horizontal area equal to $b \cdot \Delta x$, the horizontal area contained between each pair of transversal sections. This parameter is subtracted at each integration time step Δt from the previously computed η value. This is equivalent to withdrawing a water volume $b \cdot \Delta x \cdot \delta$

at each integration time step Δt . The suitable value of δ for each pair of transversal sections is determined together with the validation of the advection and dispersion model, as explained in section 3.2.”

Lines 360-372 (revised manuscript version)

“Considering that the intensity, spatial location, and temporal variability of these withdrawals are unknown, the numerical models had to undergo an ad hoc experimental validation for each campaign (MG1, MG2, MG3, and MG4). As mentioned before, for each numerical integration, an initial salt concentration field was defined using a logistic function that was determined by the behavior of the observations. The procedure begins by establishing a δ value in the hydrodynamic model, running the model, and later using the resulting u and η outputs in the advection and dispersion model to fit the salinity observations. The value of δ was determined empirically through sensitivity analysis until the best-fitting simulation was obtained.

The experimental validation determined that the best fitting of the simulated salinity values to the observations are those presented in the following lines. In MG1, a constant sink $\delta = 0.0015$ mm was implemented in all sections and time steps. For MG2, $\delta = 0.0005$ mm was applied uniformly from 0 km to 22 km and from 42 km to 85 km. From 22 km to 42 km it was increased to $\delta = 0.0045$ mm. In MG3 and MG4, a uniform sink of $\delta = 0.00225$ mm and $\delta = 0.0012$ mm was employed throughout all the sections, respectively. The slightly higher sinks between 22 km to 42 km for MG2 can be justified by the location of crop fields (Fig. 1a) and secondary channels.”

Minor comments:

- 1. Authors mention mooring observations are used. Are MG1, MG2 and MG3 mooring locations or sampling points for ship? Are the mooring observation integrated with the ship-based data? It may be good to mark the moorings in Fig. 1 and mention the location in the caption. The validation of model results using mooring observations is not shown. It may also be good to add a scatter plot between near-surface salinity from moorings and 2 m salinity from ship-based thermosalinograph data to see how they compare.**

Thank you for the comment. You are absolutely right.

The data referred to as mooring observations are the fixed stations of the thermosalinograph, whose data is recorded at a depth of 2 m depth and corresponds to the points indicated in figure 1a of the manuscript. We have changed "mooring" to "fixed station" to avoid confusion. Similarly, following your suggestion, we have added the figures we mentioned in comment 1 to the supplementary materials.

This figure demonstrates how salinity observations recorded at different depths (CTD salinity profiles) at the same locations as the fixed stations (see Fig. 1a of the manuscript) show homogeneity throughout the entire water column, with very small vertical gradients (which is in agreement with the literature). This allows us to demonstrate several aspects: the strong vertical mixing of the water column, which results in very small vertical salinity gradients, thereby helping us understand the insignificant differences between surface concentration and bottom concentration. Therefore, validation of the model can be performed using the thermosalinograph observations at 2 meters. These figures will be added to the manuscript as supplementary material SM1, SM2 and SM3 (only the points coinciding with the thermosalinograph fixed stations and presented in figure 1a of the manuscript). We will adjust the nomenclature of the other

supplementary material figures in the text to ensure that they are in the correct order. We have added these lines to the text:

Line 180 (in the revised version)

“CTD profiles obtained at the same sampling stations as the thermosalinograph data for campaigns MG1, MG2 and MG3 shown in Figure 1a are also used. These profiles are used to analyze the vertical behavior of the water column.”

Lines 275-278 (revised manuscript version)

“The salinity profiles obtained from the CTDs show a strong vertical mixing of the water column throughout the whole period and at all points (see Figures SM1, SM2 and SM3). Very reduced vertical salinity gradients can be observed, which allows us to conclude that the vertical behavior of the water column in the GRE is homogeneous under these conditions, allowing the use of a 1D model to simulate the salinity concentration along the river.”

2. Fig.1c , y-axis label needs to be corrected to “width”

Done, thank you for catching that mistake

3. Line 37: Not sure what the word “positive” means in this context.

We use positive because, GRE is a positive estuary [Elliot and McLusky, 2002], in which the freshwater discharges from the basin are sufficient to compensate evaporation losses.

We have modified the text (Lines 37-38) as follows:

“The Guadalquivir River Estuary (GRE) (Fig. 1) is a positive estuary, in which the freshwater discharges from the basin are sufficient to compensate evaporation losses (Diez-minguito et al., 2013). It is generally considered a well-mixed estuary, though this characteristic can change during periods of high discharge, when mixing conditions deviate from the typical pattern (Álvarez et al., 2001).”

4. Lines 48 and 50: m3/s should be m³/s. Superscript missing in the units in several other places. Please correct.

Thank you, we have corrected all of them.

5. Fig. 4 – It is not clear if this model simulation includes sink term or not. Also, please mention in the caption what the contours represent. How does the salt intrusion differ during the spring and neap tidal cycles before and after including the sink term? It may be worth checking that.

Thanks for the suggestion.

Figure 4 shows the 15-day simulation corresponding to the MG3 campaign, which is the campaign with the highest number of observations along the river. This allows a solid and reliable validation of the simulation. The simulation includes the parameter δ , as it is essential to reproduce the observed salinity concentrations. Without this parameter, the simulations do not reproduce the observed salinity concentrations. As seen in Figure 3, without this parameter, the horizontal salinity gradient is limited to the first 25-30 km from the mouth (using 5 psu isohaline as the limit), which is inconsistent with the observed salinity concentrations along the estuary, where 5 psu isohaline is close to 60km from the mouth.

We have modified lines 456-459 to clarify this point:

“Once the reliability of the model had been confirmed by the results of the experimental validation presented in the previous sections, it was used to simulate the dynamic of the saline intrusion during a spring-neap tidal cycle. To do this, we conducted a simulation extended over 15 days (15/07/2022-30/07/2022) using the same model configuration presented in section 3.1 for the MG3 campaign.”

In Figure 4, the contours represent the different isohalines, showing the variations in salinity along the river under different tidal conditions. We have included this information in the caption.

To improve the precision of the analysis and ensure greater clarity in the results, both the figure and the text of section 3.3 have been revised. This section is now presented as section 3.4, utilizing the updated model configuration. Moments of spring and neap tides have been selected instead of the intermediate tides previously used, enabling a more accurate and comprehensible analysis.

The section has been rewritten in alignment with all the reviewers' comments. Figure 4 now is Figure 5.

“3.4. Tidal cycle dynamics.

Once the reliability of the model had been confirmed by the results of the experimental validation presented in the previous sections, it was used to simulate the dynamic of the saline intrusion during a spring-neap tidal cycle. To do this, we conducted a simulation extended over 15 days (15/07/2022-30/07/2022) using the same model configuration presented in section 3.1 for the MG3 campaign. This period was selected because it comprised records of observations distributed throughout the spring-neap tidal cycle, allowing for the validation of the simulations. A spin-up of 3 days is necessary to stabilize the initial conditions and achieve realistic outputs.

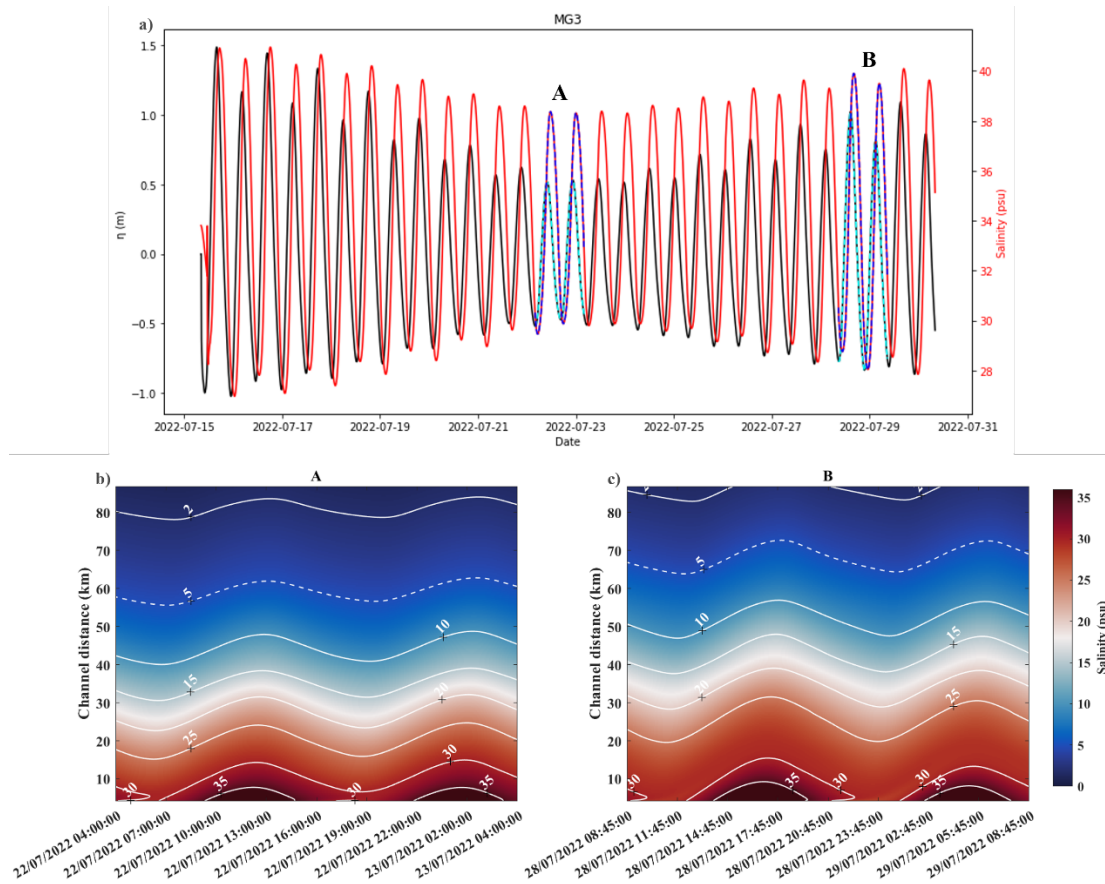


Figure 5: (a) Superposition of tidal height (m) and salinity (psu) simulated time series at Bonanza section throughout 15 days of July 2022. Dashed lines indicate the selected 24 h periods referred to in Figs. 4b and 4c; Hovmöller diagrams of simulated salinity variation over these two daily cycles (24 h) during neap tides (A) and Spring tides (B). Isohalines are presented as white lines.

We focused on two 24-hour periods to describe the dynamics of the horizontal salinity gradient during different phases of the semi-diurnal cycle (Fig. 5a). To account for water volume In Figure 5a, it can be observed that the maximum salinity levels occur near the high-water slack, while the minimum salinity levels are recorded around the low water slack. Figure 5b shows the progression of the saline intrusion during neap tides (A). Using the 5 psu isohaline as the boundary for the horizontal salinity gradient, it can be seen that the maximum salinity extends up to 63 km from the mouth, while the minimum values of this isohaline do not exceed 56 km. In contrast, during spring tides (B) (Figure 5c), as expected, higher salinity values are observed throughout all sections of the estuary compared to neap tides. The 5 psu isohaline extends up to 72 km from the mouth, while the minimum values do not exceed 65 km. This shows a difference of approximately 5-8 km between the moments of maximum and minimum intrusion, being this displacement higher for spring tides than neap tides.

In the same way, when comparing the behavior during spring tides to neap tides, we can observe a difference of 8 km between the minimum values and up to 10 km between the maximum values. Therefore, there is an oscillation of approximately 10 km between spring and neap tides. During spring tides, the horizontal salinity gradient reaches higher concentrations further upstream compared to neap tides, where both the maximum and minimum salinity values are lower. This finding is consistent with the results suggested by Díez-Minguito et al. (2013), who documented a net displacement of approximately 10 km between spring and neap tides.

These results suggest that the constant anthropogenic pressure on the estuary has caused a change in saline intrusion, resulting in higher salinity levels upstream of the river compared to the records of previous studies, such as that of Fernández-Delgado et al. (2007). In this study, it was found that over a six-year period (1997–2003), the 5 psu isohaline boundary was located near 25 km at low tide and at 35 km at high tide. The 18 psu isohaline limit was also found to be 5 km and 15 km upstream of the river mouth at low and high tides, respectively.”

6. Fig. 5 – Is this the model surface salinity plotted? Please mention the depth of salinity in the caption. Also, change the legend label in panels (b) and (d) to F +50% Q=18 m³/s

Thank you for your comment. The salinity represented in the model is the depth average. Because this is a well-mixed estuary, salinity concentrations at different depths do not show significant differences (please see CTD profiles in comment 1). Therefore, using a single vertical point is representative of the entire water column. In this case, since it is a one-dimensional model, the only point considered is the depth average.

We have modified this Figure (now is Figure 6) legend, see new figure in comment 3

7. Fig. 6 – Use the same y axis limits for panels (a) and (b).

Thank you, done.

8. Line 249-250: The November 2023 results are not shown in Fig. 2

Our apologies for the mistake, it was not November. It has been corrected

Line 388 (revised manuscript version)

The October 2023 observations show

9. Line 300: may have “an impact” on the salinity wedge penetration

Done, now it reads as follows, thank you very much:

“On the other hand, the existence of these sinks reveals ~~the significant impact~~ that the usage of water, such as those demanded by the adjacent crop fields or other domestic needs, may have an impact on the horizontal salinity gradient.”

10. Line 396: What is 2.5 psu difference? Is it the difference between the slopes of the two lines? Also, in what distance regime?

It is the maximum difference observed when using a flow rate of $Q=40\text{ m}^3/\text{s}$ compared to the original flow rates (MG2, $Q=12\text{ m}^3/\text{s}$; MG3, $Q=8\text{ m}^3/\text{s}$), considering all points in space.

But the text corresponding to this figure has been changed accordingly o the new results.

11. Line 446: through idealized model setup

Thank you for your suggestion. However, we would like to clarify that our reference is to the conceptual framework of the experiments rather than the model setup itself. To enhance clarity, we have rewritten the sentence as follows:

“The experiments conducted, based on idealized conditions, provide insight into the magnitude of anthropogenic pressures on the salinization of the GRE”